Analysis of ARMPS2010 Database with LaModel and an Updated Abutment Angle Equation

Deniz Tuncay
Ihsan Berk Tulu
Department of Mining Engineering, West Virginia University

Ted Klemetti
NIOSH Pittsburgh Mining Research Division

ABSTRACT

The Analysis of Retreat Mining Pillar Stability (ARMPS) program was developed by the National Institute for Occupational Safety and Health (NIOSH) to help the U.S. coal mining industry to design safe retreat room and pillar panels. ARMPS calculates the magnitude of the in-situ and mining-induced loads by using geometrical computations and empirical rules. In particular, the program uses the "abutment angle" concept in calculating the magnitude of the abutment load on pillars adjacent to a gob.

In this paper, stress measurements from U.S. and Australian mines with different overburden geologies with varying hard rock percentages were back analyzed. The results of the analyses indicated that for depths less than 650 ft, the ARMPS empirical derivation of a 21° abutment angle was supported by the case histories; however, at depths greater than 650 ft, the abutment angle was found to be significantly less than 21°. In this paper, a new equation employing the panel width to overburden depth ratio is constructed for the calculation of accurate abutment angles for deeper mining cases.

The new abutment angle equation was tested using both ARMPS2010 and LaModel for the entire case history database of ARMPS2010. The new abutment angle equation to estimate the magnitude of the mining-induced loads used together with the LaModel program was found to give good classification accuracies compared to ARMPS2010 for deep cover cases.

INTRODUCTION

In the early 1990s, the Analysis of Longwall Pillar Stability (ALPS) was introduced by Mark (1990) as a chain pillar design software and was generally accepted and used by the U.S. coal mining industry. Following the success of ALPS, the National Institute for Occupational Safety and Health (NIOSH) developed the Analysis of Retreat Mining Pillar Stability (ARMPS) program for designing retreat mining pillars using a similar approach as ALPS (Mark and Chase, 1997). The Australian mining industry also recognized the success of ALPS, and Colwell, Frith, and Mark (1999) calibrated the program to Australian conditions. The ALPS and ARMPS programs draw their strengths from the large databases that are used to calibrate them (Mark, 2009). However, following the Crandall Canyon Mine collapse in 2007, NIOSH had to reconsider the pillar design criteria used in deep-cover retreat mining (Mark, 2010). The ARMPS overburden load prediction algorithm was improved to more accurately predict the loading of narrow panels with high overburden depths by implementing the pressure arch concept, and this new version is called ARMPS2010.

The LaModel program is generally used in the U.S. coal mining industry to model the stresses and displacements for complex mine geometries, multiple-seam coal mines, and topographic relief which cannot be analyzed accurately by ARMPS2010 or ALPS. LaModel is a displacement-discontinuity (DD) variation of the boundary element method, and because of this formulation, the program is able to analyze large areas of single- or multiple-seam coal mines (Heasley, 1998). LaModel is unique among boundary element codes because the overburden material includes lithologic laminations which give the model a very realistic flexibility for stratified sedimentary geologies and multiple-seam mines. Using LaModel, the total vertical stresses and displacements in the coal seam are calculated. Following the Crandall Canyon Mine collapse in 2007, Heasley et al. (2010) emphasized the importance of calibrating a numerical model. It was stated that the accuracy of the input parameters greatly affects the success and accuracy of a LaModel analysis. Default properties provided by LaModel for the input parameters are applicable for average mining conditions and were developed to give reasonable results. However, site-specific conditions should be considered, and the default parameters should be modified if necessary. The first approximation of the overburden load is calibrated to mirror those used in ALPS and ARMPS2010, which were the best available information; however, the flexure of the laminated overburden and the relative stiffness/strength of the seam elements ultimately determine the final distribution of the overburden load (Heasley et al., 2010). Also, a previous study by Tulu and Heasley (2012) showed that the laminated overburden

model calculated larger abutment extents compared to the original ALPS equation.

Using the LaModel calibration method with a relatively small deep-cover database, the LaModel program was shown to classify the case histories slightly better than ARMPS2010 (Tulu, Heasley, and Mark, 2010). The analysis for the laminated model was conducted by a program called ARMPS-LAM, which has the laminated overburden model integrated with ARMPS2010. ARMPS-LAM takes the basic geometric input like that of ARMPS2010 and develops, grids, and runs a LaModel analysis of the mining geometry. It outputs the section stability factor (SF) without the requirement for further user input. Comparison between ARMPS2010 and ARMPS-LAM has been investigated by Zhang, Heasley, and Agioutantis (2014), and it was concluded that the ARMPS-LAM was more successful for shallow cover cases with less than 1,000 ft. Both ARMPS2010 and ARMPS-LAM are used in this study to check the performance of the newly suggested abutment angle equation.

ABUTMENT ANGLE CONCEPT

The abutment angle concept is used to calculate the magnitude of abutment loading adjacent to a gob area in the ALPS and ARMPS programs. LaModel also utilizes similar calculations as part of its calibration process because the abutment angle equations were determined as the best available methods for estimating abutment loads. LaModel considers an angle between the vertical plane and the panel roof in order to calculate the transferred load to the abutments when the panel is mined (Figure 1).

In 1990, Mark analyzed the abutment stress measurements collected from five different mines. All measurements were conducted using vibrating wire stressmeters (VWS). The U.S. Bureau of Mines conducted three of the studies, all of which were conducted in the Pittsburgh seam. The fourth study was conducted by the Pennsylvania State University in the Lower Kittanning seam, and U.S. Steel conducted the fifth study at a mine operating in the Harlan seam. Mark (1987, 1992) back-calculated the measured side abutment load by multiplying the load-bearing area of the pillars by the average pillar stresses determined from the array of stress cells inside each pillar. A summary of the panel widths and depths from the case histories that were used by Mark (1990) to back-calculate the abutment angles from the case histories is shown in Table 1. Originally, a total of 16 stressmeter arrays were installed in five different mines, but side abutment measurements were available only from six arrays due to some of the meters being destroyed

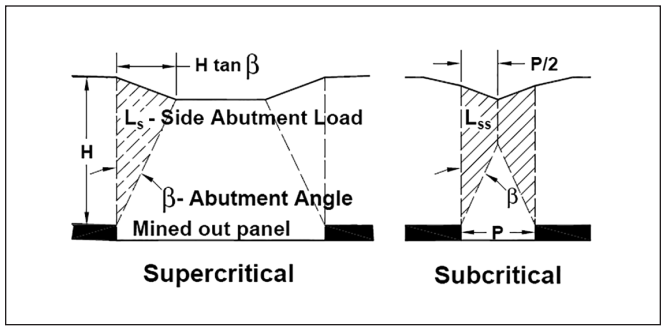

Figure 1. Abutment angle concept (Mark, 1992).

Table 1. Summary of the stress measurement sites used by Mark (1990).

Case	Panel Depth (ft)	Panel Width (ft)	Seam	Abutment Angle (deg.)
Mine A:2	520	470	Pittsburgh	21.8
Mine B:2	650	600	Pittsburgh	25.2
Mine B:3	600	600	Pittsburgh	10.7
Mine B:4	455	600	Pittsburgh	17.3
Mine D:1	760	1,000	Lower Kittanning	18.5
Mine E:3	630	500	Harlan	20.3
			Average	18.97

once the longwall had passed an array. That is why Table 1 only has data from four different mines. Mark (1992) concluded that an average abutment angle of 21° would yield a conservative estimate of the side abutment load, but there was a wide range (10.7° to 25.2°) in the measured values as seen in Table 1.

Currently, active mines have significantly different panel dimensions as compared to the mines where the data were collected for the derivation of the abutment extent formula and the 21° average abutment angle. More recent in-situ stress measurements of abutment loading conducted in Australia (Colwell, Frith, and Mark, 1999) and in the United States (Vandergrift and Conover, 2010) showed that there can be significant deviations in the measured abutment magnitude and extent, as compared to the predicted values from the present empirical formulas used in ALPS, ARMPS, and LaModel. In addition, the presence of massive stiff units, their thickness, and their location within the strata plays an important role on load transfer. Massive stiff units can transfer loads to higher distances by resisting caving, hence reducing the expected loading of the gob (Lawson et al., 2017; Reed, Mctyer, and Frith, 2017). In a study conducted by Van Dyke, Su, and Wickline (2018), it was found for their case that, within the first 50 ft of roof, presence of a more than 40 ft thick sandstone would be too strong to cave. Another factor mentioned in the study was the caving height which would have direct effect on the cushioning of the massive sandstone above. Both factors are governed by the geology of the roof layers which would affect the load distribution around the panels. Recent studies show that site-specific overburden geology, seam thickness, and extraction panel width have a significant effect on the extent and magnitude of the abutment load, but these parameters are not included in the empirical calculations.

RE-ANALYSIS OF ABUTMENT ANGLE

Stress Measurements Database

The cases used to derive the default 21° abutment angle have significantly narrower panel dimensions and relatively shallower overburden depths than most modern longwall panels. The original empirical abutment formulas were derived from the stress measurements collected from these mines and have not been updated to include the changes in mine dimensions. In this paper, more recent in-situ stress measurements are used to re-examine abutment loads with consideration of geology.

Table 2. Summary statistics of the present stress measurement database.

	Depth of Cover (ft)	Panel Width (ft)	Width / Depth
Average	950	625	0.83
Standard Deviation	518	144	0.43
Minimum	410	345	0.29
Maximum	2,050	1000	2.2

Table 1 shows that the recommended abutment angle was calculated from measurements from panels shallower than 760 ft, with most panels 600 ft wide or less.

To re-examine the abutment angle, a database was developed with the addition of more recent stress measurements. Six stress measurement case histories from Colwell, Frith, and Mark (1999) and another six case histories from Hill (2016) were added to the database. In addition to those cases and the ones studied by Mark (1990), another ten supplementary cases (Colwell, Frith, and Mark, 1999) were added where only the total side abutment loads were known. Twenty of the 28 additional case histories are from Australian longwall mines, and the remaining 8 cases are from U.S. longwall mines. Table 2 shows the statistical summary for the 28 case histories used in this study.

GEOLOGICAL SETTINGS AND MINING GEOMETRIES

Out of the 28 cases, 12 cases that have the full side abutment measurements have been further analyzed. Of those 12 cases, 10 are from different mines. One is operated in the U.S., and the other nine are operated in Australia. Geologic core logs were available for 8 of the mines and more information on the geology was gathered from consulting reports.

Figure 2 shows the generalized stratigraphic columns of the case study sites, where enough information was present about the geology. Layers with more than one rock type represent interbedded or intermixed components, but the percentages may vary. Also, thick layers do not necessarily represent massive rock formations. Adjacent thin layers of the same rock types are combined for easier representation.

The available core logs and descriptions of the geologies from the reports were used to determine the hard rock percentage (%HR) of the overlying strata for each case. Hard rock percentage is calculated considering the thickness of hard rock (sandstone and limestone) that is higher than 5 ft from the core log (Agioutantis and Karmis, 2017). It is the ratio of the length of hard rock core that is longer than 5 ft to the total length of the core log above the coal seam. This methodology for defining the hard rock percentage was originally developed by Agioutantis and Karmis (2017) and used successfully in predicting subsidence magnitude and profile for the U.S. coal mines. The following is a list of the case studies with the mine geometries and available geologic information, and Table 3 show the summary of the cases.

AU1 Mine

The AU1 mine's coal seam varies in thickness from 5.9 to 8.9 ft. The overlying strata mostly consists of sandstone and laminate units. Enough information was not available to construct a representative stratigraphic column; however, the geologic formations that were present in the immediate roof were known. The depth of cover around the instrumentation site is approximately 870 ft. The chain pillars are developed on 148-ft × 328-ft centers with a 16.7-ft entry width and the panel is 673 ft wide. The immediate floor is strong with minimum slaking potential. There were no stratigraphic data to determine the hard rock percentage of the overlying strata.

AU2 Mine

The AU2 mine operates with a seam thickness from 9.5 to 13.8 ft, and the seam thickness is approximately 11.8 ft at the monitoring site. The stratigraphic sequence can be seen in

Figure 2. A sandstone and siltstone unit overlies the coal seam. A thick clay unit overlies a clay/sand sequence followed by a varying thickness of basalt. The overburden depth above the instrumentation site is around 410 ft. The panel width is 920 ft and the chain pillars are on 115-ft × 427-ft centers with 16.4 ft entry widths. The hard rock ratio is calculated as 48% for this mine.

AU3 Mine

The seam thickness for the AU3 mine varies from 11 to 13 ft, and a typical stratigraphic column near the instrumentation site is presented in Figure 2. The seam is overlain mostly by sandstone with a couple of bands of siltstone and claystone. The hard rock percentage is calculated as 57%. The depth of cover is approximately 427 ft, and the panel void width is 673 ft. The chain pillars are on 98-ft × 410-ft centers with 17-ft-wide roadways. There is a 3.3-ft thick clayey siltstone underlying the coal seam that deteriorates when exposed to water and traffic, so 1.7 ft of coal is left for maintaining good roadway conditions. Below the clayey siltstone, the lithology continues with strong layers of sandstone, shale, mudstone and siltstone.

AU4 Mine

At the AU4 mine, 15.7 ft of coal is extracted. The overlying strata consists of layers of generally competent and strong layers of shale, sandstone, conglomerate, volcanic tuff and coal seams (Figure 2). The depth of cover varies from 490 to 660 ft where it is approximately 590 ft at the instrumentation site. The 444-ft-wide longwall panels are designed with 102 ft × 335 ft center chain pillars with 16.4 ft wide roadways. The hard rock ratio is around 33%. The floor of the seam mostly consists of sandstone with occasional thin shale units in some areas.

AU5 Mine

The seam extracted at the AU5 mine is relatively flat and 8.2 ft in thickness. Overlying the seam, there is a 984-ft-thick sequence of major sandstone and shale units. That sequence is overlain by a massive sandstone of 525 to 590 ft of thickness.

Figure 2 has the visual representation of the stratigraphic column; however, it is generated from the description of the geology in a report without a core log. The overburden is approximately 1,560 ft above the instrumentation site and can be considered 71% hard rock. The 673-ft-wide panels are supported by 138-ft × 335-ft center chain pillars, and the roadway width is approximately 15.7 ft. The immediate floor is around 3.3 ft of carbonaceous siltstone underlain by a strong sandstone.

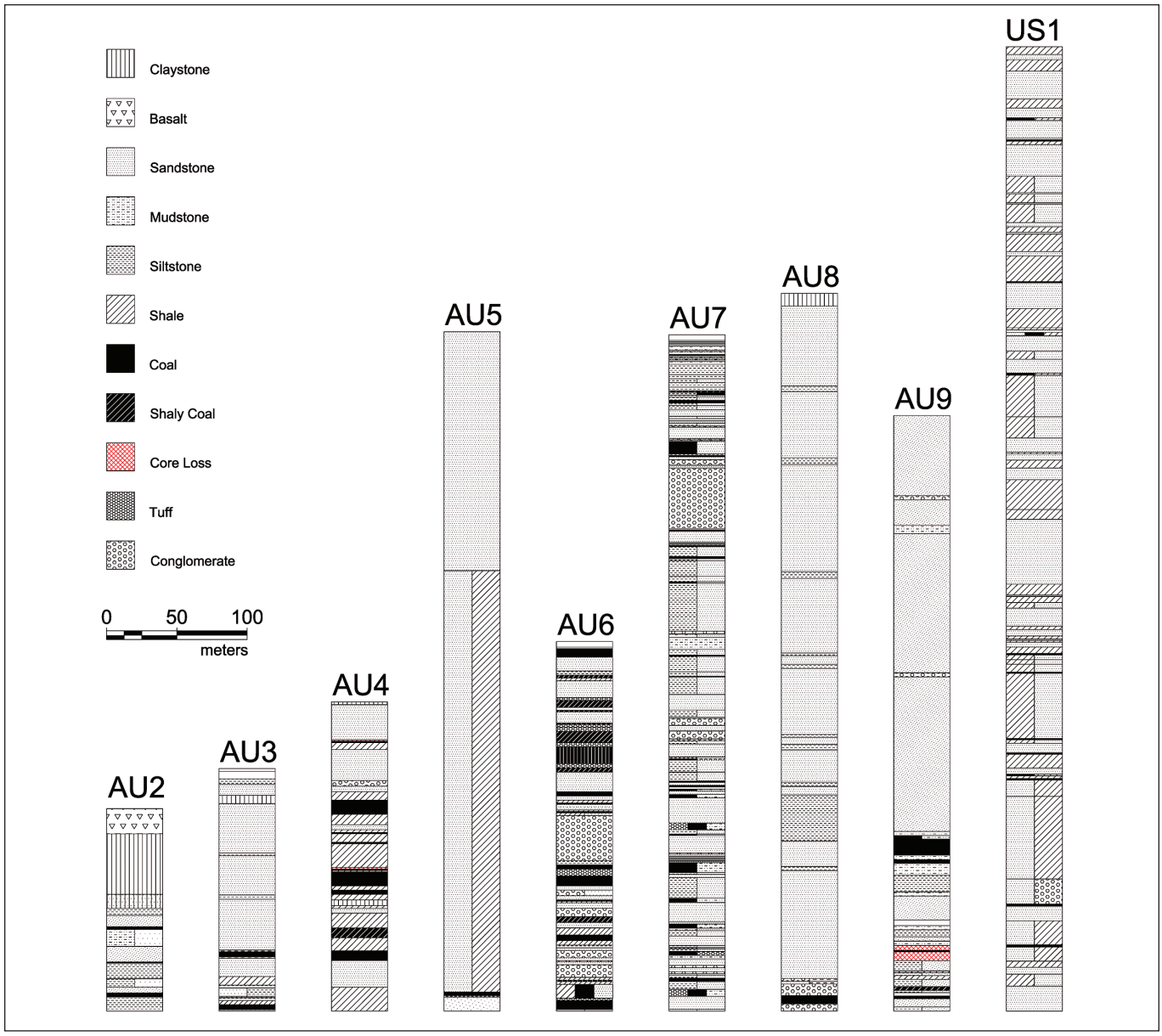

Figure 2. Generalized stratigraphic column representation of the mines.

AU6 Mine

The coal seam at the AU6 mine is 21.3-ft thick, but the development thickness is 10.5 ft. Immediately overlying the seam is a competent volcanic tuff layer of 4.9-ft thickness. Sequence of shale and sandstone layers follow with some minor coal seams. There is a very strong sandstone/conglomerate unit lying 50–60 ft above the roof (Figure 2). The depth of cover varies from 720 to 920 ft with 787 ft adjacent to the instrumentation site with around 23% hard rock. The 492-ft-wide panels are separated by chain pillars on 115-ft centers with 16-ft-wide roadways. The immediate floor is 13-ft-thick shale underlain by inter-bedded sandstones and shales.

AU7 Mine

The AU7 mine operates at a depth of cover of 1,330 ft with a variable seam thickness from 5.9 to 12 ft. The panel widths are 656 to 820-ft wide (rib to rib), and they are supported by 158-ft-wide chain pillars, which have 17-ft-wide nominal cut-throughs at 328-ft centers. The overlying strata mostly consist of sandstone intermixed or interbedded with siltstone (Figure 2) that produced about a 21% hard rock ratio.

AU8a-b Mine

Two sets of measurements were taken from the AU8 mine. The depth of cover changes from 1,640 to 1,755 ft. The seam thickness varies from 16.4 to 21.7 ft. The overlying strata mostly consists of thick sandstone layers and siltstone giving a 72% and 95% hard rock ratio, respectively (Figure 2). The immediate floor and roof have conglomerate units. The measurements are taken next to two different panels that are 745- and 778-ft wide. Chain pillars are 148 ft wide with 16.4 ft wide entries for the 745-ft-wide panel and for the 778-ft-wide panel, the chain pillars are 197-ft-wide with 20-ft-wide entries.

Table 3. Summary of mine geometries for the new cases.

Case	Depth (ft)	Panel Width (ft)	Seam Thickness (ft)	Entry Width (ft)	HR%
AU-1	870	673	8.2	16.7	-
AU-2	410	920	11.8	16.4	48%
AU-3	427	673	10.2	17	57%
AU-4	590	444	10.5	16.4	33%
AU-5	1,560	673	8.2	15.7	71%
AU-6	787	492	21.3	16	23%
AU-7	1,330	820	8.2	17	21%
AU-8a	1,683	745	18	16.4	72%
AU-8b	1,673	778	18	20	95%
AU-9	1,197	820	22	16.4	61%
US-1a	1,950	640	5.5	20	54%
US-1b	2,050	600	5.5	20	54%

AU9 Mine

The depth of cover for the AU9 mine typically ranges from 984 to 1,148 ft. A sandy soil cover of 3 to 16-ft depth overlies a low to very low strength, highly weathered sandstone on the surface. Highly competent and massive sandstone units exist between depths of 165 to 655 ft (Figure 2). The panel extracted adjacent to the instrumentation site is 820-ft wide with an extraction height of 22 ft, and the chain pillars are 141 ft wide, rib to rib with 16.4-ft-wide roadways. The hard rock ratio is calculated as 61%.

US1a-b

Two sets of measurements are collected from the US1 mine where the overburden depths were 1,950 and 2,050 ft, respectively. The panels are supported by 20-ft-wide yield pillars on both sides of 80-ft-wide chain pillars. First measurements are taken next to a 640-ft-wide panel, while the other set of measurements are collected next to a 600-ft-wide panel. The hard rock ratio of the overlying strata was calculated as 54%. The strength and stiffness of the surrounding strata of the coalbed are uncommonly high for coal measure rocks. Except for the dark-gray shale, all the rock types have uniaxial compressive strength (UCS) values from 28,590 to 17,500 psi. The absence of roof and floor fractures or joints together with the thick sandstone result in hard-to-break main roof and greater pillar loads at this site (Campoli et al., 1993).

ABUTMENT ANGLE ANALYSIS

Back-Calculation of Abutment Angles

In-situ stress measurements constitute the stress profiles. A sample stress profile plotted using the measured values can be seen in Figure 3. The figure represents the stress change profile of a two-entry system where the measurements are taken from the pillars and the adjacent solid coal. The area L_A represents the abutment load on the gateroad pillar, and the area L_B represents the abutment load on the adjacent solid coal. The areas L_A and L_B were numerically calculated by integrating the load under the curve.

Tulu and Heasley (2012) have explained the back-calculation for laminated overburden stress distribution approach in detail, and the same procedure is used for calculating the abutment loads for this study.

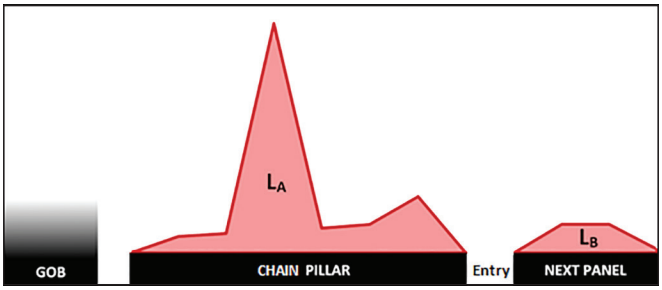

Figure 3. Sample stress profile from a two-entry mine.

Table 4. Back-calculated abutment angles.

Case	Abutment Angle	Overburden Depth (ft)	Panel Width (ft)
AU-1	23.39	870	656
AU-2	19.30	410	900
AU-3	17.24	425	656
AU-4	16.03	590	425
AU-5	6.33	1,560	656
AU-6	11.79	787	475
AU-7	12.48	1,330	820
AU-8a	13.62	1,680	745
AU-8b	8.85	1,673	778
AU-9	10.00	1,197	820
US-1a	9.51	1,950	640
US-2b	8.74	2,050	600

Finally, the value of the abutment angle is back calculated from the ratio of abutment load to total panel load according to the subcritical or supercritical panel formulas. Considering available subsidence information to determine the panel condition (subcritical or super critical) will give a more precise result. When enough information was present, it was taken into account in this study.

The back-calculated abutment angles can be seen in Table 4. The results showed that for deeper mines, the abutment angle was lower than the average 21° abutment angle used in ALPS and ARMPS2010.

Regression Analysis for Abutment Angle

Next, the hypothesis that there was a correlation between the geology and the abutment angle was tested. Figure 4 shows the calculated abutment angles with respect to panel width to overburden depth ratios, with the hard rock percentages as color coding. The blue points represent the cases that have hard rock ratios higher than 80 percent, and the yellow points represent the cases that have hard rock ratios between 50 and 80 percent. The red points represent the cases with less than 50 percent hard rock in the overlying strata. There was not any apparent significance of the percentage hard rock on the abutment angle. The only visible finding was some clustering of stronger overburden cases at lower

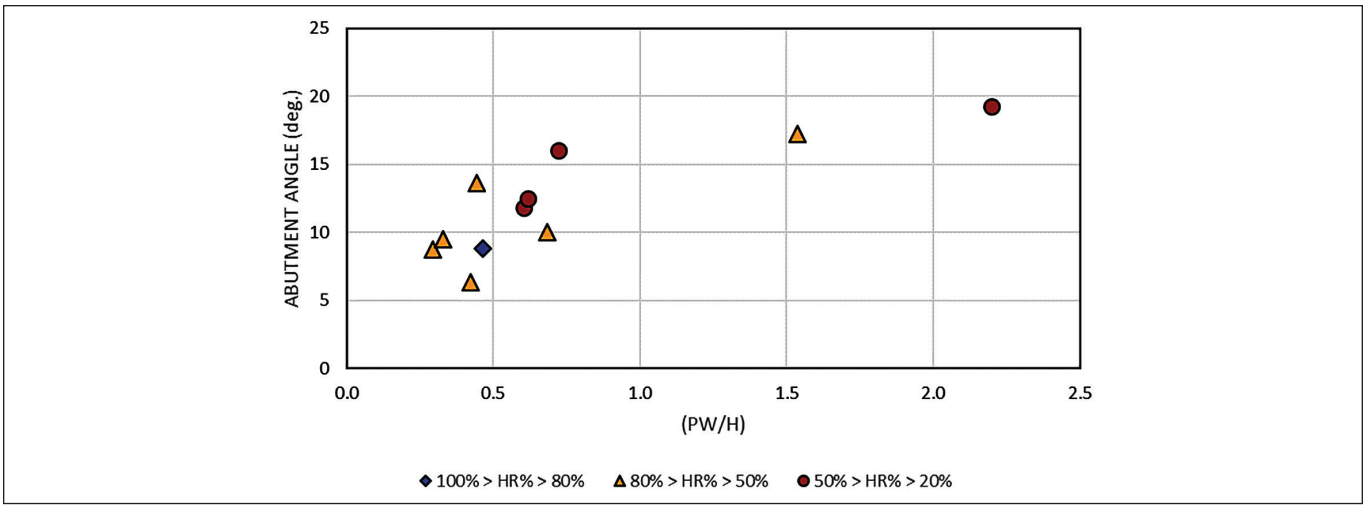

Figure 4. Abutment angles calculated using laminated model with respect to panel width to overburden depth ratio together with hard rock percentages.

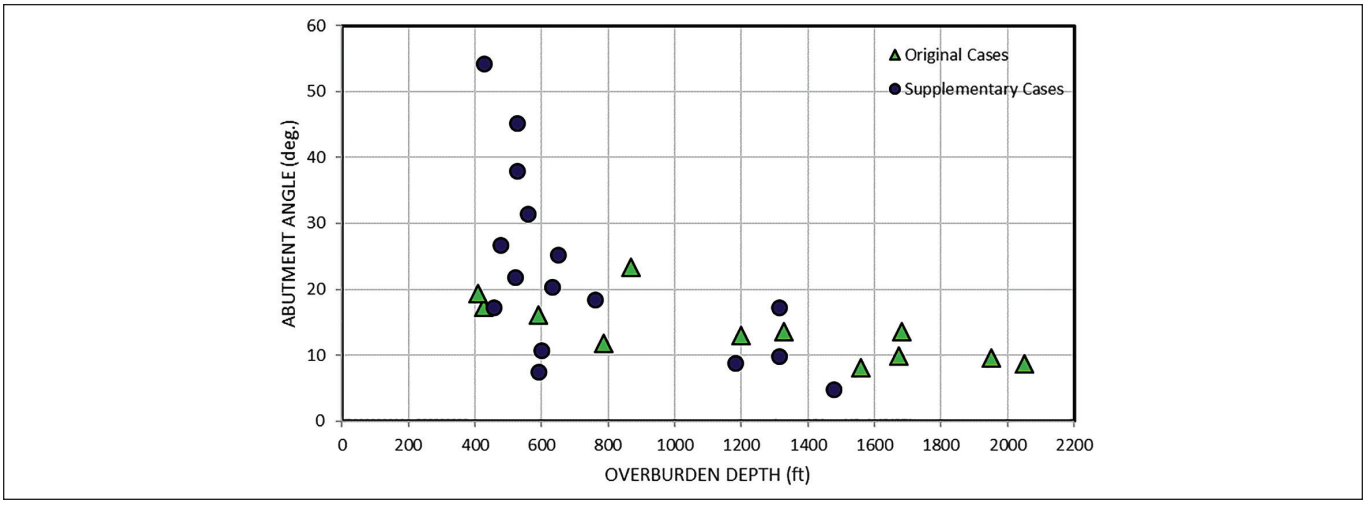

Figure 5. Determined abutment angles with respect to overburden depth.

abutment angles. More comprehensive geological analysis with additional geological information is needed for a better conclusion.

Figure 5 shows the results for the abutment angles back-calculated using the laminated model together with previously calculated cases (Colwell, Frith, and Mark, 1999; Hill, 2016; Mark, 1990). For the mines deeper than 650 ft, the abutment angle values are distributed from the maximum value of 23.4° to the minimum value of 4.7°, with the mean of 12.2°. For the mines with overburden depth less than 650 ft, the scatter is much larger, but the average abutment angle of 21° is appropriate to assume.

As seen in Figure 6, there is also an apparent trend of decreasing abutment angle with increasing ratio of overburden depth to panel width (H/PW). A regression analysis to determine the abutment angle for deep cover cases (> 650 ft) is conducted. The 650 ft is selected as the limit depth, since the large data scatter occur for shallower cases. Also, the value is reasonable to be considered as the boundary between deep and shallow mines (Mark, 2010).

For the regression analysis, the H/PW ratio was found to be the most significant parameter for determining the abutment angle, and the following equation is proposed:

$$\text{Abutment Angle} = a \times b^{\left(H/PW\right)} \quad (1)$$

Based on the field data analyzed in this paper, the proposed abutment angle determination is shown as the red line in Figure 7. When the overburden depth is less than 650 ft, a constant abutment angle of 21° is still applicable. With an overburden depth from 650 ft to 2,050 ft, researchers in this study propose an abutment angle (β) that decreases with a continuous function of the H/PW ratio is proposed (Table 5). This equation was derived by performing a least-square error fit to the measured abutment angles above 650 ft overburden depth. Almost all the cases deeper than 650 ft also have an H/PW ratio more than 1. The new equation should be considered applicable inside the range of the case studies ($0.7 < (H/PW) < 3.5$).

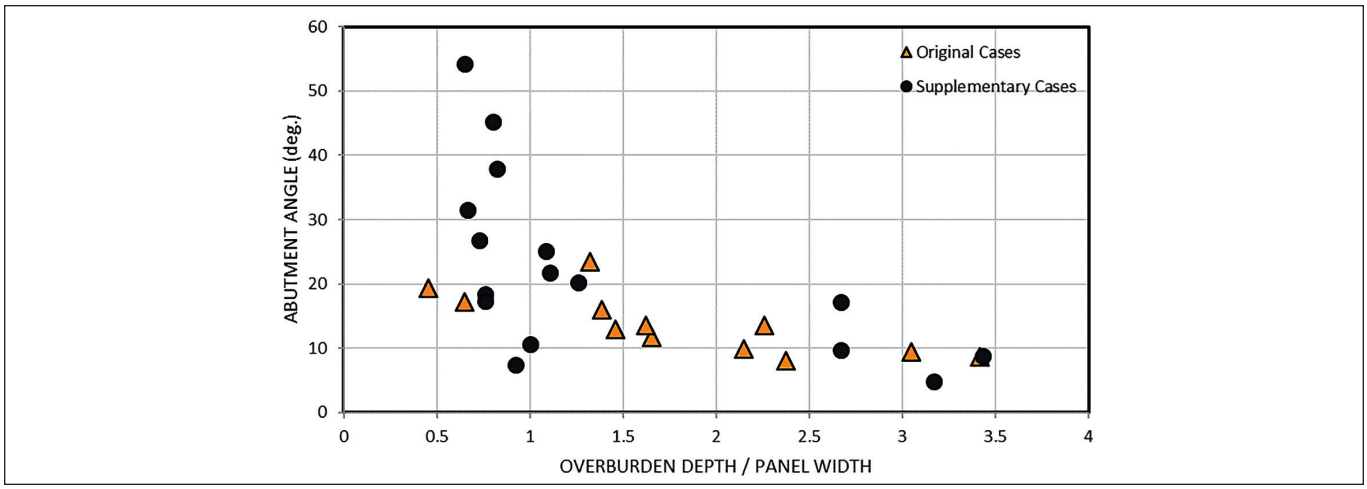

Figure 6. Determined abutment angles with respect to panel width to overburden depth ratio.

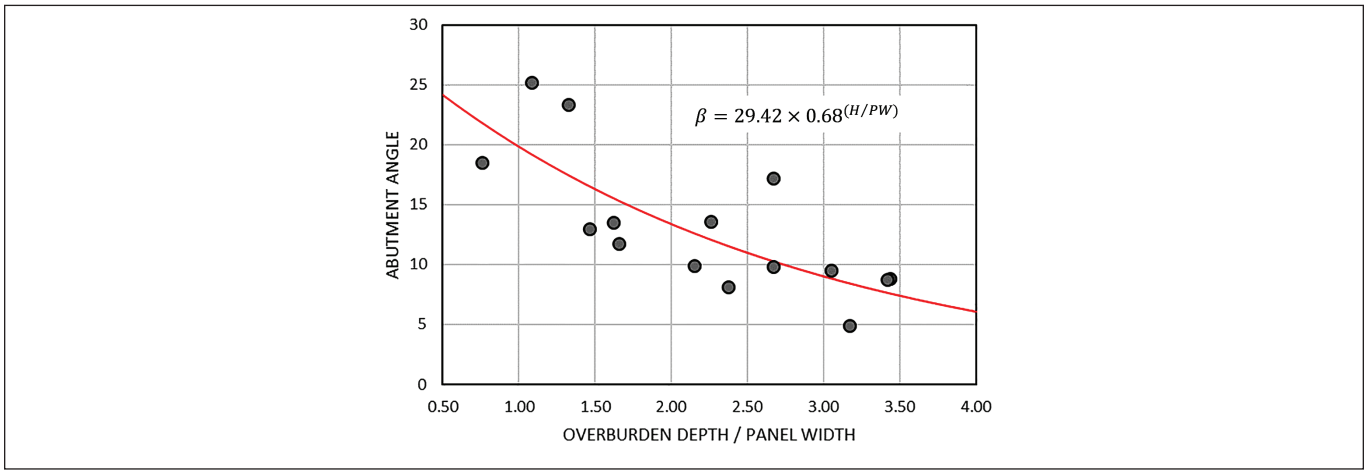

Figure 7. New abutment angle model for deep cover cases.

Table 5. Proposed abutment angle equation for H/PW ratios from 0.7 to 3.5.

Overburden Depth (H)	Abutment Angle (deg.)
H ≤ 650 ft	21°
650 ft ≤ H ≤ 2,050 ft	$\beta = 29.42 \times 0.68^{(H/PW)}$

LOGISTIC REGRESSION ANALYSIS FOR DATABASE CLASSIFICATION

In order to confirm its applicability, the new abutment angle equation was tested on the case histories that were used for the development of the ARMPS2010 design criteria. The stability factors for 640 cases were calculated using both the ARMPS2010 and ARMPS-LAM programs. The database used for the analysis includes 640 cases, of which 520 were successful and 120 are failed case histories. The failed cases include: 14 collapses, 81 squeezes, 16 multipillar bursts, and 9 local bursts. The analyses aimed to compare the new abutment angle equation with the classification success of the ARMPS2010 design criteria. The failure classification rates of the ARMPS2010 design criteria are matched and compared.

First, shallow cases (<650 ft) are tested considering the ARMPS2010 design criteria of ARMPS2010 SF of 1.5. The ARMPS2010 SF refers to the stability factor of the pillars inside the active mining zone (AMZ) as a whole. The ARMPS2010 classification rates are given in Table 6. Of the 204 shallow cases, 46 of them are failed cases with 28 squeezes and 14 pillar collapses. Out of the 46 failed cases, ARMPS2010 design criteria successfully predicted 42 of them (91.3%). The 4 failed cases that are predicted falsely include only pillar squeezes. The 133 of the 158 (84%)

Table 6. Classification accuracies of ARMPS2010 SF of 1.5 for shallow mines using 21° abutment angle.

	Success Observed	Failure Observed	Total
Success Predicted	133	4	137
Failure Predicted	25	42	67
Total	158	46	204
Accuracy	0.84	0.91	0.86

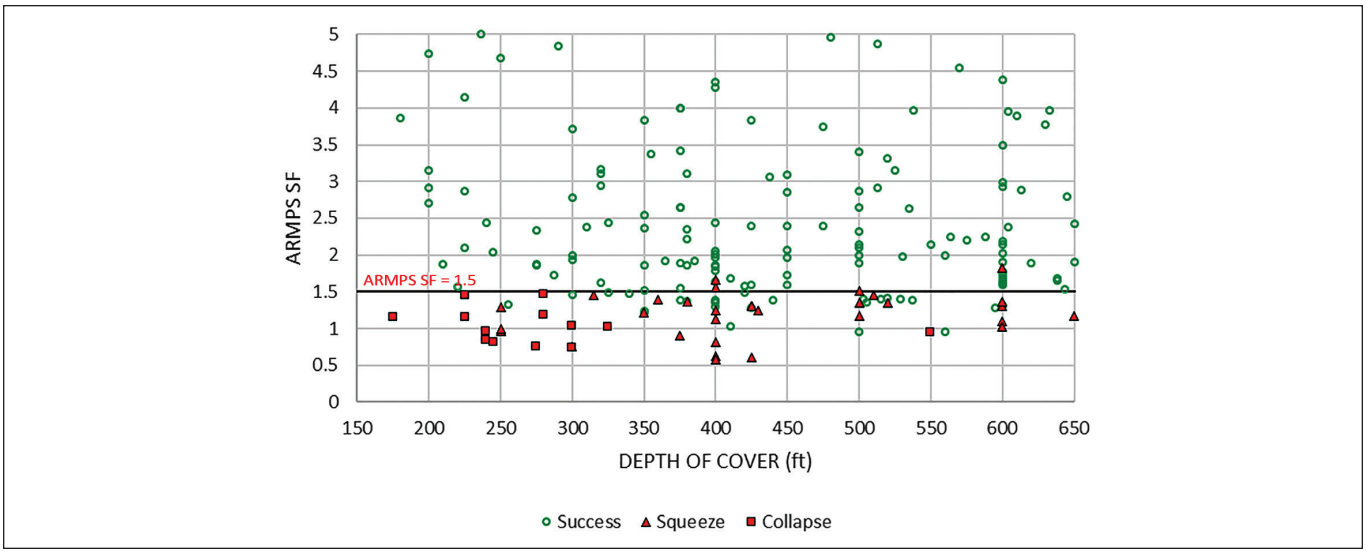

Figure 8. ARMPS2010 SF results of the ARMPS2010 shallow cover (< 650 ft) database using the 21° abutment angle.

successful cases were also predicted correctly by the design criteria (Figure 8).

Stability factor values for the same case histories were also calculated by ARMPS-LAM using the new abutment angle equation. Since the new abutment angle equation was proposed for deep cover cases, both programs used the original 21° abutment angle. The limit SF value was determined as 1.84, so that the classification accuracy of failed cases is set to be 91.3%, the same as the ARMPS2010 classification accuracy. This suggests that if one uses ARMPS LAM for design purposes, 1.84 should be taken as the limit stability factor. The results are given in Table 7. The classification accuracy of the successful cases were slightly reduced from 84% down to 83%. Also, one pillar collapse and three pillar squeezes (Figure 9) were predicted falsely compared to ARMPS2010 that only misplaced pillar squeezes. It can be concluded that, for shallow cases, almost identical separation was achieved with the ARMPS-LAM program.

A second set of analyses were conducted using the 215 deep cover case histories that utilize barrier pillars. Out of those 215 cases, 182 of them were successes and the remaining 33 were failures. These cases were initially analyzed using 21° abutment angle and standard ARMPS2010 design criteria that use 1.5 for both ARMPS2010 SF and barrier pillar stability factor (BP SF) values. Corresponding classification accuracies are given in Table 8. The ARMPS2010 design criteria correctly predicted 29 of 33 failures (88%) and 61 of 182 successful cases (34%). Out of the 4 falsely predicted cases, one of them was a local pillar burst, and the other three were pillar squeezes (Figure 10).

The same case histories (deep cover with barrier pillars) are re-analyzed using the ARMPS2010 program with the new abutment angle equation (Table 5) instead of the constant 21°. In order to provide with a failure classification accuracy of 88%, the ARMPS2010 SF was kept as 1.5 and BP SF value is determined as 2.15. As seen in Table 9, classification of successful cases increased notably up to 43% (78 out of 104). Failure types of the falsely predicted failed cases remained unchanged (1 local burst, 3 squeezes).

Both AMZ and BP SF values were calculated for the same 215 cases using ARMPS-LAM with the abutment angle calculated with the new suggested equation. A minimum of 88% accurate failure classification is targeted for the limit SF values to be considered. That classification accuracy is achieved with an AMZ SF of 1.45 and BP SF of 2.2. 88% failure classification accuracy is achieved with a success classification accuracy of 46% (Table 10).

As seen in Figure 11, ARMPS-LAM only misclassified pillar squeezes, where ARMPS2010 design criteria misclassified a local burst failure in addition to pillar squeezes. Although pillar squeezes cause hazardous situations, the fact that they develop slowly (where collapses and bursts occur with little or no warning) makes it easier to react to the situation and abandon the area (Mark, 2010).

Table 7. Classification accuracies of ARMPS-LAM SF of 1.84 for shallow mines using 21° abutment angle.

	Success Observed	Failure Observed	Total
Success Predicted	131	4	135
Failure Predicted	27	42	69
Total	158	46	204
Accuracy	0.83	0.91	0.85

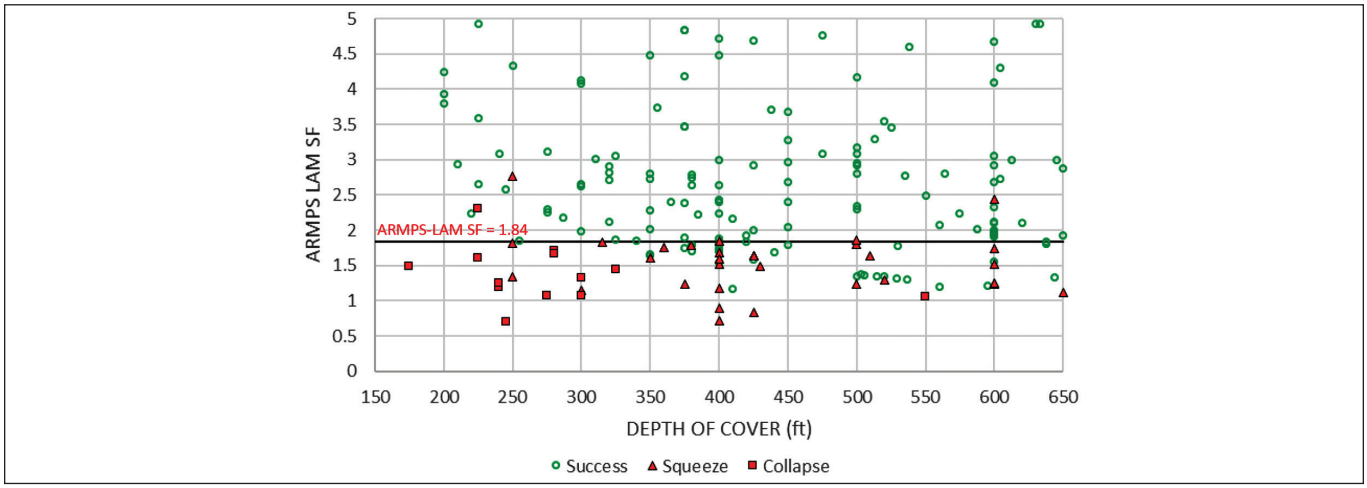

Figure 9. ARMPS-LAM SF results of the ARMPS2010 shallow cover (< 650 ft) database.

Table 8. Classification accuracies for deep cover cases of ARMPS2010 SF and the BP SF of 1.5 using the 21° abutment angle.

	Success Observed	Failure Observed	Total
Success Predicted	61	4	65
Failure Predicted	121	29	150
Total	182	33	215
Accuracy	0.34	0.88	0.42

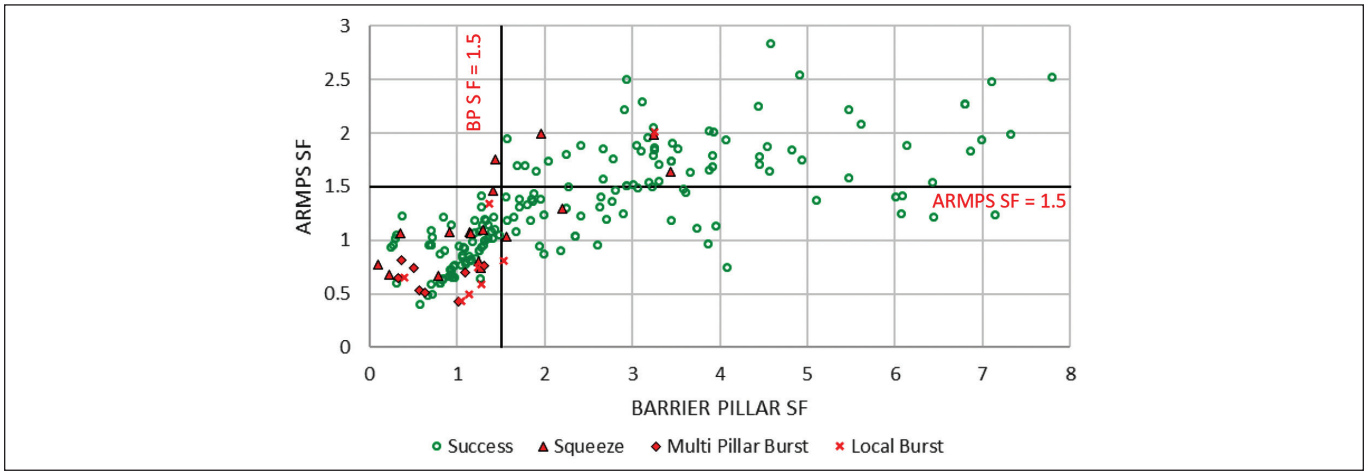

Figure 10. ARMPS2010 SF values for deep cover cases that utilize barrier pillars using 21° abutment angle.

Table 9. Classification accuracies for deep cover cases using the new abutment angle equation using the ARMPS2010 program with ARMPS2010 SF. 1.5 and BP SF. 2.15.

	Success Observed	Failure Observed	Total
Success Predicted	78	4	82
Failure Predicted	104	29	133
Total	182	33	215
Accuracy	0.43	0.88	0.50

Table 10. Classification accuracies for deep cover cases of ARMPS-LAM SF of 1.45 and BP SF of 2.2 using the new abutment angle equation.

	Success Observed	Failure Observed	Total
Success Predicted	84	4	88
Failure Predicted	98	29	127
Total	182	33	215
Accuracy	0.46	0.88	0.53

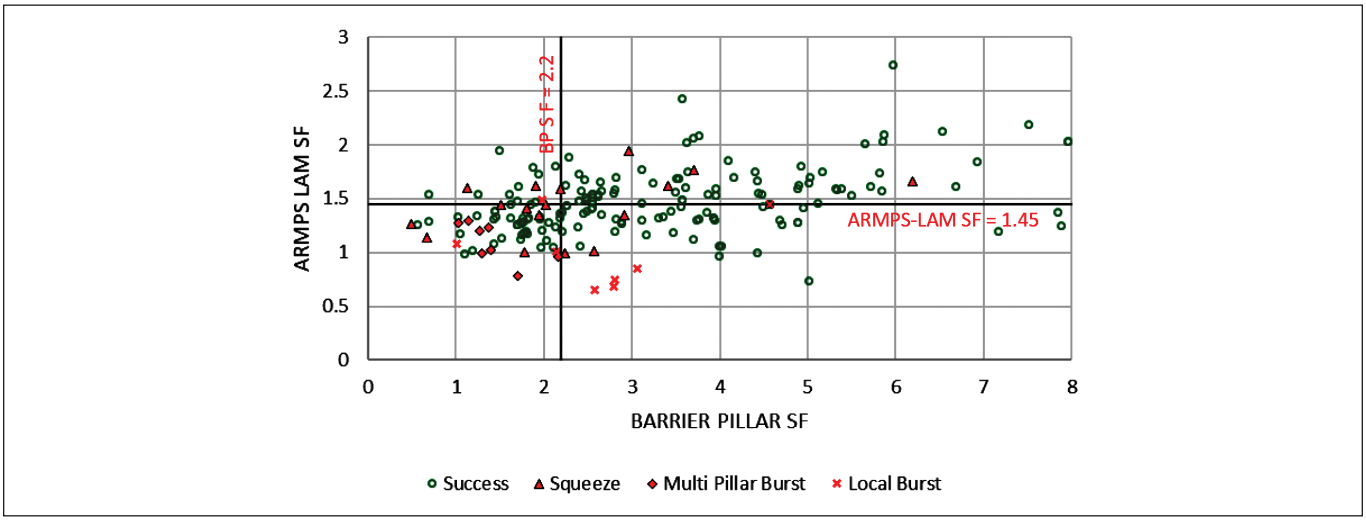

Figure 11. ARMPS-LAM classification capability for deep cover cases using the new abutment angle equation.

Table 11. ARMPS2010 and ARMPS-LAM classification accuracies for different sets of cases.

			ARMPS2010	ARMPS-LAM
	No. of Cases	Failure Classification Accuracy	Success Classification Accuracy	Success Classification Accuracy
All Cases	640	82.5%	59.0%	55.0%
Shallow Cover Cases	204	91.3%	84.1%	82.9%
Deep Cover Cases	436	94.7%	16.8%	23.1%
Deep Cover Cases with Side Gob	249	92.0%	30.7%	42.2%
Deep Cover Cases with Barrier Pillar	215	87.9%	33.5%	46.2%

In Table 11, the classification accuracies of both ARMPS2010 and ARMPS-LAM for different cases are presented. The failure classification accuracy of ARMPS-LAM was targeted to be at least as good as that of ARMPS2010 for the same cases. More than 80% of the cases that utilize barrier pillars are deep cover cases, so we can say that ARMPS-LAM, used together with the new abutment angle equation, gives considerably better results for deep cover cases. Since the shallow cover cases are not included in the new abutment angle equation, those can be considered for the comparison of ARMPS2010 and ARMPS-LAM.

For deep cover cases, ARMPS LAM SF of 1.45 and BP SF of 2.2 was found to be applicable when the new abutment angle equation is used together with the laminated model. However, if ARMPS LAM is used for shallow cover cases, the limit ARMPS LAM SF should be taken as 1.84.

SUMMARY AND CONCLUSIONS

The ARMPS2010 design software for retreat mining pillar design uses the empirically derived abutment angle of 21° that was derived from field studies conducted in the mid-1980s and 1990s (Mark, 1992; Peng and Chiang, 1984). Modern mine designs use significantly different panel depths and widths compared to these cases. In this paper, traditional calculations for abutment loading are re-examined using a current database of more recent in situ

stress measurements from 12 full case studies with an additional 18 supplementary case studies.

The re-analysis of the abutment angles presented in this paper showed that for higher overburden depths, the re-analyzed abutment angle appears to be much less than the traditionally used 21° abutment angle. Based on the field data analyzed in this paper, researchers propose a new abutment angle calculation that considers depth to panel width ratio (see Table 5). When the overburden depth is less than 650 ft, the 21° abutment angle proposed by Mark (1992) still holds its applicability. It is known from the ARMPS2010 analysis that the 21° abutment angle works fine for the shallow cover cases (Mark, 2010). However, from depths of 650 to 2,050 ft, the abutment angle calculated with the equation in Table 5 should be considered.

Using the proposed new abutment angle equation, cases used to develop ARMPS2010 were re-analyzed with the ARMPS-LAM software. It was observed that the ARMPS2010 design criteria was slightly better at classifying the cases when the shallow cover database is considered. However, when the deep cover cases are considered separately, the classification accuracy of ARMPS2010 is improved with the newly proposed abutment angle equation. If the deep cover cases with a barrier pillar are considered separately, 88% of the failed cases and 46% of the successful cases were correctly predicted by ARMPS-LAM compared to using a constant 21° abutment angle (88% and 34%, respectively). It can be concluded that, for deep cover cases, a better separation can be achieved by the new abutment angle equation. Also, the ARMPS-LAM program gave better separation for deep cover cases and was almost equally successful when shallow cover cases were considered. The fact that ARMPS-LAM provides a real mechanical explanation for the load transfer is an important factor to be considered in mine layout design. ARMPS-LAM software can be considered as a design tool, especially for deep cover (> 650 ft) cases that use barrier pillars with the implementation of the newly proposed abutment angle equation. For deep cover cases, ARMPS LAM SF of 1.45 and BP SF of 2.2 was found to be applicable when the new abutment angle equation is used together with the laminated model. However, if ARMPS LAM is used for shallow cover cases, the limit ARMPS LAM SF should be taken as 1.84.

Finally, in this study, there was no apparent relationship between the hard rock ratio and the abutment angle, which might be due to insufficient information about the overlying strata. Since there is no doubt that the overburden geology plays an important role on load distribution around the panels, a more comprehensive investigation with detailed geological information is planned to be conducted in the future.

REFERENCES

Agioutantis, Z., & Karmis, M. (2017). *Quick reference guide and working examples, SDPS for Windows, version 6.2J.*

Campoli, A., Barton, T., Van Dyke, F., & Gauna, M. (1993). *Gob and gate road reaction to longwall mining in bump-prone strata.* Report of Investigations 9445 (Bureau of Mines).

Colwell, M., Frith, R., & Mark, C. (1999). Analysis of longwall tailgate serviceability (ALTS): a chain pillar design methodology for Australian conditions. *Proceedings of the 2nd International Workshop on Coal Pillar Mechanics and Design* (pp. 33–48). NIOSH: IC 9448.

Heasley, K. (1998). *Numerical modeling of coal mines with a laminated displacement-discontinuity code.* Golden (CO): Colorado School of Mines.

Heasley, K., Sears, M., Tulu, I., Calderon-Arteaga, C., & Jimison II., L. (2010). Calibrating the LaModel program for deep cover pillar retreat coal mining. *Proceedings of the 3rd International Workshop on Coal Pillar Mechanics and Design*, (pp. 47–57). Morgantown WV.

Hill, D. (2016). Personal communications.

Lawson, H., Tesarik, D., Larson, M., & Abraham, H. (2017). Effects of overburden characteristics on dynamic failure in underground coal mining. *International Journal of Mining Science and Technology*, 121–129.

Mark, C. (1987). *Analysis of Longwall Pillar Stability.* PhD Dissertation: The Pennsylvania State University.

Mark, C. (1990). *Pillar design methods for longwall mining.* IC 9247: U.S. Bureau of Mines.

Mark, C. (1992). Analysis of Longwall Pillar Stability (ALPS): an update. *Proceedings of the Workshop on Coal Pillar Mechanics and Design* (pp. 238–249). U.S. Bureau of Mines.

Mark, C. (2009). Deep cover pillar recovery in the U.S. *Proceedings of the 28th International Conference on Ground Control in Mining*, (pp. 1–9). Morgantown WV.

Mark, C. (2010). Pillar design for deep cover retreat mining. *Proceedings of the 3rd International Workshop on Coal Pillar Mechanics and Design*, (pp. 106–121). Morgantown WV.

Mark, C., & Chase, F. (1997). Analysis of retreat mining pillar stability. *Paper in New Tech. for Ground Control in Retreat Mining: Proceedings of the NIOSH Technology Transfer Seminar* (pp. 17–34). NIOSH IC 9446.

Peng, S., & Chiang, H. (1984). *Longwall Mining.* Wiley & Sons.

Reed, G., Mctyer, K., & Frith, R. (2017). An assessment of coal pillar system stability criteria based on a mechanistic evaluation of the interaction between coal pillars and the overburden. *International Journal of Mining Science and Technology*, 9–15.

Tulu, I., & Heasley, K. (2012). Investigating abutment load. *Proceedings of the 31st International Conference on Ground Control in Mining*, (pp. 28–37). Morgantown WV.

Tulu, I., Heasley, K., & Mark, C. (2010). A comparison of the overburden loading in ARMPS and LaModel. *Proceedings of the 29th International Conference on Ground Control*, (pp. 150–159). Morgantown WV.

Van Dyke, M., Su, W., & Wickline, J. (2018). Evaluation of seismic potential in a longwall mine with massive sandstone roof under deep overburden. *International Journal of Mining Science and Technology*, 115–119.

Vandergrift, T., & Conover, D. (2010). Assessment of gate road loading under deep western U.S. conditions. *Proceedings of the 3rd International Workshop on Coal Pillar Mechanics and Design*, (pp. 38–46). Morgantown WV.

Zhang, P., Heasley, K., & Agioutantis, Z. (2014). A Comparison Between ARMPS and the New ARMPS–LAM Programs. *33rd International Conference on Ground Control in Mining*, (pp. 170–174). Morgantown WV.

PROCEEDINGS OF THE 38th International Conference ON GROUND CONTROL IN MINING

ICGCM 2019

Edited by

Ted Klemetti | Brijes Mishra | Heather Lawson | Michael Murphy | Kyle Perry

Published by the
Society for Mining, Metallurgy & Exploration

Society for Mining, Metallurgy & Exploration (SME)
12999 E. Adam Aircraft Circle
Englewood, Colorado, USA 80112
(303) 948-4200 / (800) 763-3132
www.smenet.org

The Society for Mining, Metallurgy & Exploration (SME) is a professional society whose more than 15,000 members represents all professionals serving the minerals industry in more than 100 countries. SME members include engineers, geologists, metallurgists, educators, students and researchers. SME advances the worldwide mining and underground construction community through information exchange and professional development.

ISBN 978-0-87335-472-1